band centered on ω_1 is "quenched" or prevented from growing, and adjacent unstable noise modes are limited in amplitude. Of greater interest is the case when the launched wave is (a) small enough that its amplitude grows exponentially before saturating, and (b) far enough above the initial thermal noise elvel that the launched wave always traps the beam. The exponentially growing noise is observed to be unaffected until the launched wave has trapped the beam. Curve *C* is the spectrum received at a point after the beam has been trapped by a 114-MHz wave launched where the beam enters the plasma and with an amplitude approximately 10 dB above the thermal noise level. Curve *D* is the spectrum received at the same position but with no launched wave.

The similarity between the calculation and the experimental result is evident. The principal failure of the calculation is that the observed noise amplitude in the "quenched" region ($|\omega_1 - \omega_n| < 2$ MHz) is not zero, but rather is limited to the level it had grown to before trapping. This amplitude limiting and the spatial evolution of these limited waves have been previously calculated by regarding them as a slow modulation of the launched wave's amplitude and phase.[7] It is likely that the failure is not the fault of the Van der Pol model, but rather is a result of the constant-driver approximation that facilitated the calculation.

The principal success of the model is that, unlike the modulational point of view, the Van der Pol model clearly exhibits the frequency range over which a launched wave affects the unstable modes at neighboring frequencies.

In summary, the unstable modes on a low-density, cold-electron-beam–plasma system have been treated as an ensemble of Van der Pol oscillators. Qualitative agreement is found with the observed amplitude limiting of unstable waves at the neighboring frequencies of a launched wave that has trapped the electron beam.

*Present address: Department of Applied Sciences, University of California, Davis, Calif. 95616. Work at San Diego supported by National Science Foundation Grant No. GP-27120.

†Work supported by U. S. Atomic Energy Commission Contract No. AT(40-1)3405 and U. S. Air Force Office of Scientific Research Contract No. AFOSR 72 2179.

[1]B. van der Pol, Phil. Mag. 3, 65 (1927).

[2]H. Lashinsky, in *Nonlinear Effects in Plasmas*, edited by G. Kalman and M. Feix (Gordon and Breach, New York, 1969).

[3]H. Lashinsky, in *Turbulence of Fluids and Plasmas (Microwave Research Institute Symposia–Polytechnic Institute of Brooklyn, v. 18)*, edited by J. Fox (Wiley, New York, 1969).

[4]W. E. Lamb, Jr., Phys. Rev. 134, A1429 (1964).

[5]B. E. Keen and W. H. W. Fletcher, Phys. Rev. Lett. 24, 130 (1970).

[6]Y. Nakamura, J. Phys. Soc. Jap. 31, 273 (1971).

[7]C. P. DeNeef, J. H. Malmberg, and T. M. O'Neil, Phys. Rev. Lett. 30, 1032 (1973).

[8]T. M. O'Neil, J. H. Winfrey, and J. H. Malmberg, Phys. Fluids 15, 1514 (1972).

[9]J. J. Stoker, *Nonlinear Vibrations* (Interscience, New York, 1950), pp. 149–187.

[10]E. M. Dewan, IEEE Trans. Automat. Contr. 17, 655 (1972).

Electrostatic Wave Reflection from a Plasma Density Gradient*

C. W. Roberson, A. S. Ratner, and J. L. Hirshfield
Department of Engineering and Applied Science, Yale University, New Haven, Connecticut 06520
(Received 11 June 1973)

We report measurements of the reflection coefficient R for electron plasma waves propagating into a density gradient on a narrow column. Within experimental error, R is proportional to $\exp(-\delta)$ when R is less than 0.25 and is equal to $\exp(-0.23\delta)$ for R greater than 0.25, where δ is the inverse of the WKB parameter.

Considerable theoretical effort has recently been applied to the problem of electrostatic plasma-wave reflection from plasma density gradients. One motivation for this effort has been to determine if reflections of convectively unstable waves from the ends of a mirror machine affect the stability of these devices.[1-6] The problem is also relevant to considerations of the axial boundary conditions for beam-plasma devices. In this Letter we present measurements of the reflec-

tion coefficients of small-amplitude electron plasma waves on a narrow plasma column propagating into an adjustable axial density gradient. Reflections occur because of the spatial gradient in axial wave number, and the waves are observed to extinguish substantially at a plasma density above the value corresponding to resonance. The experimental results agree favorably with the calculations of Aamodt and Book[1] in the weak-reflection limit.

The plasma was produced by a cyclotron-resonance discharge in a TE_{113} cavity driven at power levels of up to 200 W from a 2.45-GHz cw magnetron. The plasma diffused out of a 1-cm-diam hole at the end of the cavity into a chamber 15 cm in diameter and 160 cm in length. The plasma was confined radially by a uniform 800-G magnetic field which rendered the electron dynamics one-dimensional. The radial density profile was found to be Gaussian from ion saturation-current measurements with a radially movable Langmuir probe. The e-fold radius was about 1 cm, the central density approximately 2×10^{9} cm^{-3}, and the electron temperature about 5 eV. The neutral gas pressure was 3×10^{-5} Torr of argon, corresponding to an electron mean free path much greater than the machine length; hence, collisional damping was negligible. The plasma was surrounded by two 7.6-cm-diam conducting cylinders which served as a wave guide beyond cutoff for transverse waves at the frequencies used. The cylinders were separated by a 0.5-cm axial gap located 60 cm from the transmitter, a 3-cm-diam wire loop connected to the inner conductor of a rigid coaxial transmission line. The cylinder nearer the transmitter was grounded, while the farther one was biased below ground and terminated with a fine mesh grid. The bias on the second cylinder produced a static electric field which had an axial component that was uniform (within a few percent) over the diameter of the plasma column. This electric field caused an axial density gradient which could be adjusted by varying the cylinder bias. Two such axial profiles, as determined from ion saturation-current measurements with the movable axial probe, are shown in Fig. 1.

Waves on the plasma column were launched at the transmitter, and the amplitude of the wave measured as a function of distance in the vicinity of the gradient by means of an axial rf probe connected to a sampling voltmeter. Figure 2 shows recorder traces of received rf voltage versus axial position for three representative frequencies. These traces were taken using a density profile intermediate between the two shown in Fig. 1. The undulations in the traces have a periodicity which is twice the axial wavelength, as measured from interferometer patterns, and represent standing waves. The reflection coefficient was inferred from these traces by measuring the standing-wave ratio. This procedure for measuring the reflection coefficient can lead to inaccuracies due to the finite wave coherence length and to variations in wave-probe coupling in the density gradient. However, there was no evidence that these were a significant source of error in

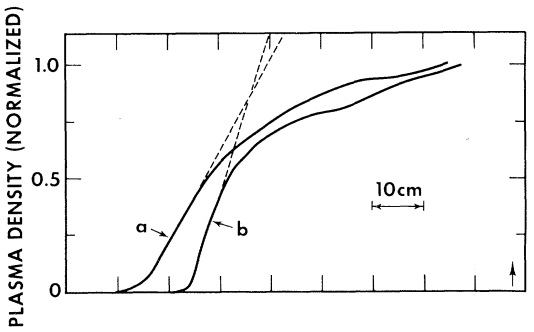

FIG. 1. Two representative axial density profiles. The cylinder bias for curve a was -70 V and for b was -200 V. The maximum plasma densities were 2×10^{9} and 4×10^{9} cm^{-3}, respectively. Dashed lines indicate the slope where the density gradients used to define δ are determined. Waves are launched from a transmitter located at a position designated by the arrow.

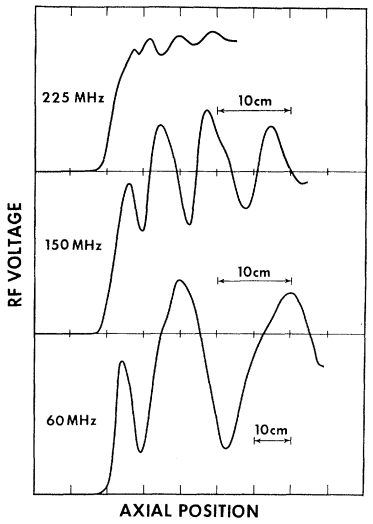

FIG. 2. Standing wave patterns. Note that the horizontal scale is compressed by a factor of 2 for the 60-MHz trace.

this experiment. At high frequencies reflections were weak and wave absorption was nearly complete. Since no wave transmission was observed in the region of minimal plasma density, one can infer that a fraction $1-R^2$ of the wave energy has been absorbed, presumably by Landau damping.

Aamodt and Book[1] have considered reflection of electrostatic waves from weak plasma inhomogenities in the fluid approximation. They find a reflection coefficient which is proportional to $\exp[-\delta(\omega)]$ for $\delta \gg 1$, where $\delta(\omega)=[k^{-2}(\omega)\,dk(\omega)/dz]^{-1}$. Here $k(\omega)$ is the local axial wave number and is related to ω through the local dispersion relation when $\delta \gg 1$.

The dispersion relation for electron plasma waves on a column with a Gaussian radial profile, surrounded by a conducting cylinder with a diameter large compared to the plasma, which is immersed in a strong magnetic field may be written as[7]

$$(1+1/ka)^2 = k^{-2}\lambda_D^{-2} Z'(\omega/kv_e), \qquad (1)$$

where $Z(\omega/kv_e)$ is the plasma dispersion function, $\lambda_D = v_e/\omega_p$ is the Debye length, ω is the wave frequency, v_e is the electron thermal speed, and a is the e-fold radius of the plasma. This dispersion relation has been compared with numerical solutions, a previous experiment,[8] and the present experiment. In all cases excellent confirmation of Eq. (1) was found in the range of experimental interest. With no bias on the cylinder we have determined the plasma density and temperature from a least-squares fit of this relation to the measured dispersion relation.

With a bias on the cylinder, reflections of waves with phase velocities such that $\omega/kv_e \gg 1$ were observed to originate near the position where the density gradient was strongest. In this limit Eq. (1) reduces to $ka=\omega/[\omega_p(z)-\omega]$, where $\omega_p(z)$ is the plasma frequency; $\delta=\omega(a\,d\omega_p/dz)^{-1}\equiv\alpha\omega$, where α is determined from measurements of the radius and density gradient at the reflection point. The radius was found to be independent of bias over the range of density gradients considered, so as to rule out variations in k with a.

Figure 3 shows the results of our reflection-coefficient measurements. Data are shown for four different density gradients, obtained by adjustment of the cylinder bias, corresponding to changes in the parameter α of over a factor of 2. The solid line is proportional to $\exp(-\delta)$ for comparison with the Aamodt-Book prediction; the amplitude was obtained by fitting to the data at one point. The apparent dependence of the

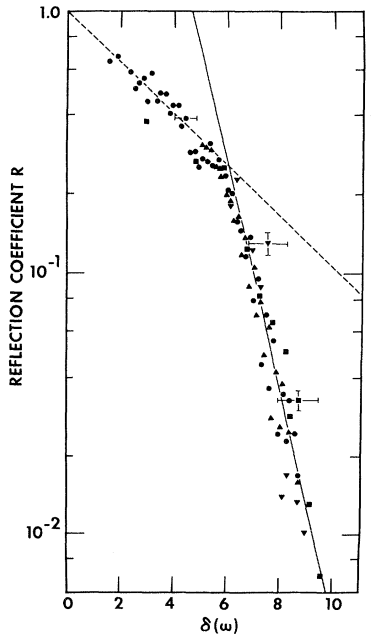

FIG. 3. Reflection coefficient. The triangles, dots, squares, and inverted triangles correspond to $\alpha = 4.6$, 5.1, 8.0, and 11.5, respectively, in units of 10^{-9} sec^{-1}.

measured reflection coefficient solely upon $\delta(\omega)$ suggests that the agreement between experiment and theory is not peculiar to a specific set of experimental conditions. For strong reflections, the dashed curve indicates an empirical fit of $\exp(-0.23\delta)$. The break between strong and weak reflections appears to be at a reflection coefficient of about 0.25. This corresponds to a WKB parameter $\delta^{-1}=0.17$ and suggests a criterion for application of the WKB approximation and a need for another theory for smaller δ. There is no evidence that nonlocal resonant-particle effects[3,5] are important here, since the phase velocity of the wave is so large that the bias on the cylinder is insufficient to reflect resonant particles.

Berk *et al.*[5] have calculated a reflection coefficient from the Vlasov equation, but their theoretical model assumes a perpendicular wave number much greater than the axial one, a condition not satisfied in the present experiment. It may not be surprising, therefore, to note that we have found very poor agreement between that theory and this experiment.

It is a pleasure to acknowledge stimulating discussions with Dr. D. E. Baldwin, Dr. J. Fukai, and Professor Ira Bernstein.

*This work was supported in part by the National

Science Foundation.

[1]R. E. Aamodt and D. L. Book, Phys. Fluids 9, 143 (1966).
[2]H. L. Berk, M. N. Rosenbluth, and R. N. Sudan, Phys. Fluids 9, 1606 (1966).
[3]D. E. Baldwin, Phys. Rev. Lett. 18, 1119 (1967).
[4]H. L. Berk, C. W. Horton, M. N. Rosenbluth, and R. N. Sudan, Phys. Fluids 10, 2003 (1967).
[5]H. L. Berk, C. W. Horton, M. N. Rosenbluth, D. E. Baldwin, and R. N. Sudan, Phys. Fluids 11, 365 (1968).
[6]H. L. Berk, L. D. Pearlstein, and J. G. Cordey, Phys. Fluids 15, 891 (1972).
[7]C. W. Roberson, Ph.D. thesis, University of Texas, Austin, 1971 (unpublished).
[8]C. W. Roberson and K. W. Gentle, Phys. Fluids 14, 2462 (1971).

Laser Target Model*

N. K. Winsor
Naval Research Laboratory, Washington, D.C. 20375

and

D. A. Tidman
Science Applications Inc., Arlington, Virginia

(Received 10 August 1973)

Results of a numerical simulation model are presented. Internally generated megagauss magnetic fields are produced which tend to impede and deform the heat flow into the target plasma beyond the laser-energy deposition layer. Two new instabilities are also discussed.

A two-dimensional code has been developed for the processes involved in the interaction of a focused laser pulse with a moderate-atomic-weight target. A system of fluid equations including self-generated magnetic fields[1-3] is solved in cylindrical geometry by a second-order algorithm using time-step-split flux-corrected transport.[4] Interest in these plasmas derives from their potential application as pulsed x-ray sources,[5] ion sources, and possibly fusion. We shall present representative results of numerical simulations, demonstrate the importance of the self-generated magnetic field, and draw attention to two instabilities which may play a role in the physics of the laser-target interaction.

Typically, we consider nanosecond (or subnanosecond) Nd pulses with intensities $>10^{14}$ W/cm^2 through the focal spot, which give rise to target plasma temperatures above 1 keV. Thermal energy spreads from the laser focal region via electron thermal conduction, fluid expansion, and line and continuum emission from highly charged ion states. Magnetic fields in the megagauss range are generated internally in the plasma and tend to inhibit thermal conduction in the direction perpendicular to $\vec{B}$ in regions where $\Omega_e\tau_e>1$. Radiation pressure also plays a role for intensities $>10^{14}$ W/cm^2, but is not included in the present code.

The fluid equations used are

$$\partial N/\partial t+\nabla\cdot(N\vec{V})=0, \tag{1}$$

$$NM\,d\vec{V}/dt+\nabla\cdot[P\overleftrightarrow{I}+\overleftrightarrow{I}B^2/8\pi-\vec{B}\vec{B}/4\pi]=0, \tag{2}$$

$$\partial\mathcal{E}/\partial t+\nabla\cdot(\mathcal{E}\vec{V})=-P\nabla\cdot\vec{V}+\vec{J}\cdot\vec{E}'+\langle\delta\vec{E}\cdot\delta\vec{J}\rangle+R_e+\nabla\cdot(\overleftrightarrow{K}_e\cdot\nabla T_e), \tag{3}$$

$$P=C_P(\mathcal{E},N),\quad T_e=C_T(\mathcal{E},N), \tag{4}$$

$$\frac{\partial\vec{B}}{\partial t}=\nabla\times\left[\vec{V}\times\vec{B}-\frac{c^2}{4\pi}\overleftrightarrow{r}\cdot(\nabla\times\vec{B})\right]-\frac{ck}{eN_e}\nabla N_e\times\nabla T_e, \tag{5}$$

where

$$\vec{E}'=\vec{E}+\vec{V}\times\vec{B}/c=-(eN_e)^{-1}\nabla(ZNkT_e)+\overleftrightarrow{r}\cdot\vec{J}. \tag{6}$$

In these equations N is the total ion number density, $\langle\delta\vec{E}\cdot\delta\vec{J}\rangle$ the laser-energy deposition term, $P=NkT(1+Z)$ the total pressure, $\mathcal{E}$ the thermal plus ionization energy density, and R_e the rate of change of $\mathcal{E}$ due to radiation processes. The resistivity $\overleftrightarrow{r}$, and electron thermal conductivity $\overleftrightarrow{K}_e$, are taken from the work of Braginskii[1] with the $\vec{B}$ dependence of $\overleftrightarrow{r}$ and $\overleftrightarrow{K}_e$ included. The coronal model[6] calculates the distribution of ion charge states assuming equilibrium between electron collisional ionization and radiative recombination. It provides P and T_e as functions C_P and